

Electronic supplementary information

EFFICIENT IN-MAGNET ^{15}N HYPERPOLARIZATION INDUCED BY REVERSIBLE EXCHANGE OF PARAHYDROGEN WITH AN Ir-BASED CATALYST

D. A. Markelov,^{*a,b} A. S. Kiryutin,^a I. D. Kosenko,^c Zh. V. Matsulevich,^d
I. A. Godovikov,^c and A. V. Yurkovskaya^a

^a International Tomography Center, Siberian Branch of the Russian Academy of Sciences, ul. Institutskaya 3A, Novosibirsk, 630090 Russia

^b Novosibirsk State University, ul. Pirogova 1, Novosibirsk, 630090 Russia

^c Nesmeyanov Institute of Organoelement Compounds, Russian Academy of Sciences, ul. Vavilova 28, str. 1, Moscow, 119334 Russia

^d Nizhny Novgorod State Technical University, ul. Minina 24, Nizhny Novgorod, 603155 Russia

Catalyst activation

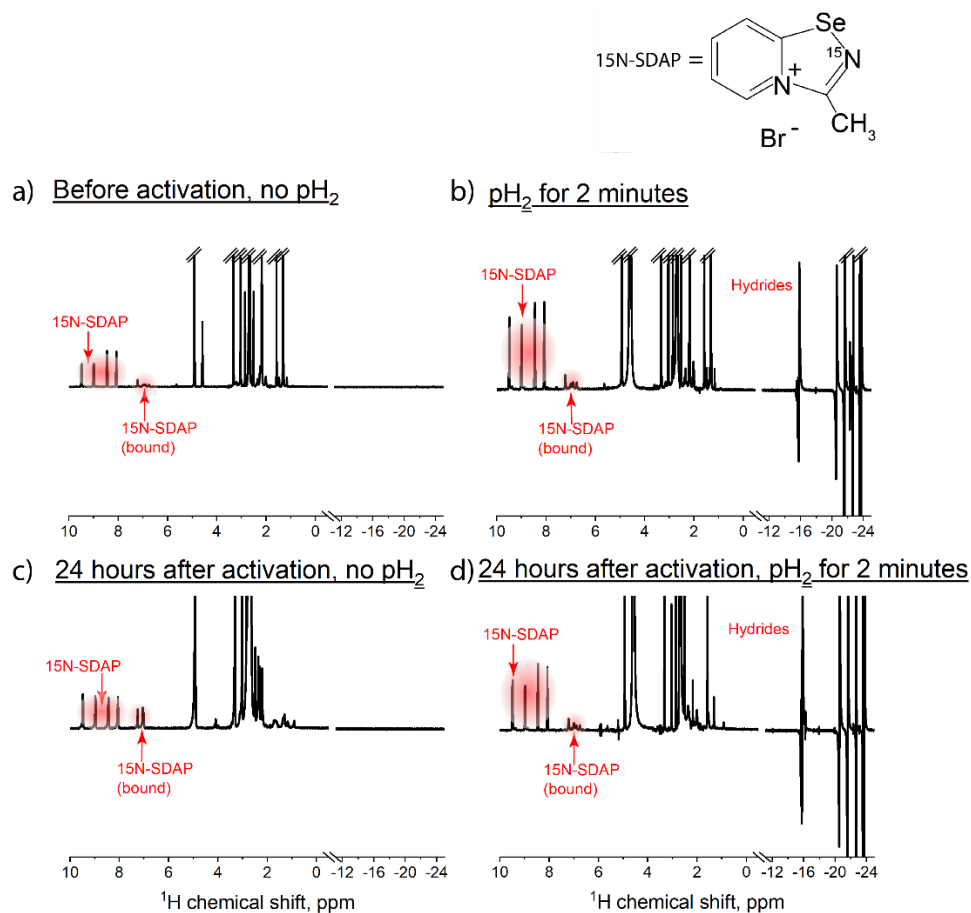


Figure S1. ^1H NMR spectra of the investigated sample with ^{15}N -SDAP. (a) Thermal NMR spectrum before parahydrogen (pH_2) bubbling; (b) hyperpolarized NMR spectrum acquired with parahydrogen bubbling for 2 min; (c) thermal NMR spectrum acquired the next day after the first parahydrogen bubbling; (d) hyperpolarized NMR spectrum of the next day pH_2 -bubbled sample. The temperature of the sample was 15° in all cases.

The first step of our experiments was the catalyst activation procedure, during which the active SABRE complexes were formed from [IrCl(COD)(IMes)]. The activation of the catalyst consisted in bubbling the sample containing the pre-catalyst and substrate with parahydrogen. The activation of the catalyst has its own kinetics and steady-state. In the steady-state, the hydride area of ^1H NMR spectrum demonstrates stable over time complexes, and subsequent parahydrogen bubbling does not lead to any changes in the ^1H NMR spectrum.

Figure S1 demonstrates the ^1H NMR spectrum of the investigated sample with ^{15}N -SDAP at different time points. Figure S1a shows the thermal NMR spectrum of the sample before bubbling. The signals from 8 to 10 ppm refer to the aromatic protons of ^{15}N -SDAP, while the signals from 6 to 8 ppm belong to ^{15}N -SDAP in the complex-bound form. The spectral range from 1 to 4 ppm is more complicated and contains the signals from the precatalyst (from COD and IMes) and from the active catalyst. The detailed analysis of these signals for a similar system at different time points can be found, for example, in Ref. [S1]. Figure S1b demonstrates the ^1H NMR spectrum obtained after 2 min of the sample bubbling with parahydrogen (catalyst activation). In this case, the hyperpolarized hydrides (from -12 to -25 ppm) are observed, and the subsequent bubbling does not change the NMR spectrum. The hyperpolarization of the hydride ^1H nuclei occurs due to the PASSADENA effect [S2].

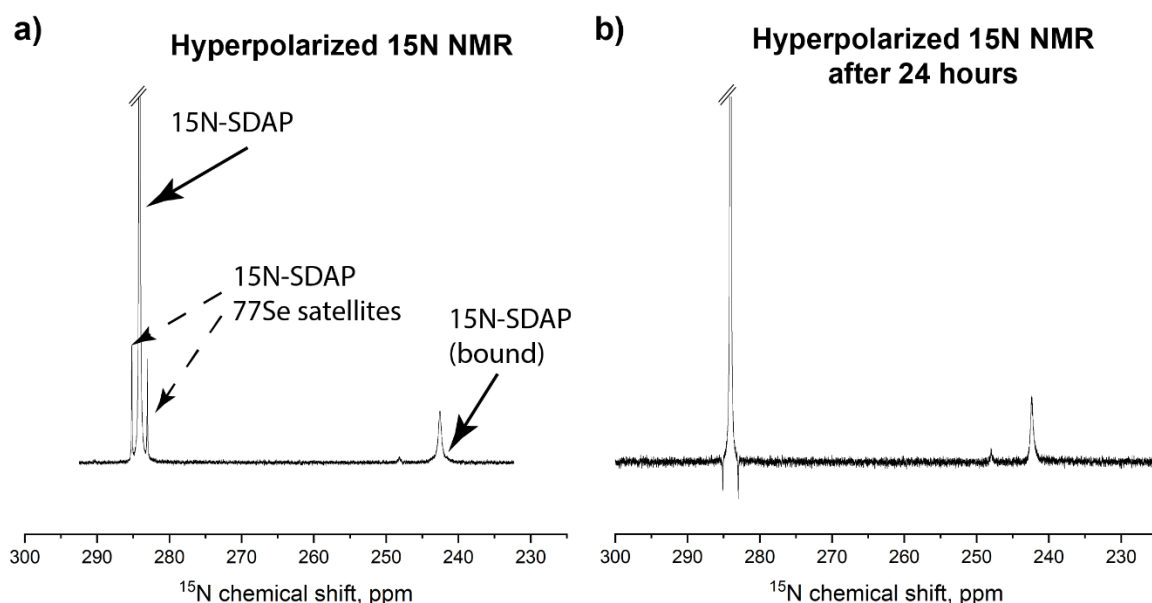


Figure S2. Hyperpolarized ^{15}N NMR spectra obtained by SABRE: (a) at the first day of the experiments, (b) the next day after the experiments.

To demonstrate the stability of the sample and the absence of hydrogenation of ^{15}N -SDAP, we also acquired the ^1H NMR spectra in 24 h after the first parahydrogen bubbling of the sample (during these 24 h, we had been conducting the SABRE experiments, and the sample was bubbled with parahydrogen for several hours). Figure 1c shows the thermal ^1H NMR spectrum acquired the next day after the first parahydrogen bubbling. No change in the intensity or position of the ^1H signals of ^{15}N -SDAP from 8 to 10 ppm is observed. Moreover, parahydrogen bubbling after 24 h leads to the formation of identical hydrides and identical ^{15}N -SDAP signals, as demonstrated in Fig. S1d (compare with Fig. S1b), and no hydrogenation products are observed in the ^1H NMR spectrum. The absence of the hydrogenation and stability of the sample can also be alternatively determined in the hyperpolarized ^{15}N NMR spectrum, where no hydrogenation products are observed after 24 h (see Figs. S2a,b). In both cases, the

hyperpolarized ^{15}N spectra contain the signals from ^{15}N -SDAP, its ^{77}Se satellites, and ^{15}N -SDAP bound to the Ir-catalyst (it should be noted that the ^{77}Se satellites in these figures have different phases because we used different SABRE protocols for hyperpolarization). The absence of the substrate hydrogenation has also been confirmed in the pioneer SABRE work [S3], where instead of the catalytic hydrogenation of a substrate, it was involved in the reversible interactions with an Ir-catalyst. Such a behavior is typical for a variety of different substrates [S4].

Optimization of the SABRE pulse sequences

The SABRE-INEPT pulse sequence requires an optimization of two time delays between the ^1H and ^{15}N pulses, denoted as τ and τ_1 . In our experiments, we used $\tau_1 = 10$ ms and optimized time delay τ , as demonstrated in Fig. S3. The maximum of the ^{15}N signal enhancement, ε , was observed at $\tau = 8.5$ ms, which we have used in the subsequent experiments with SABRE-INEPT.

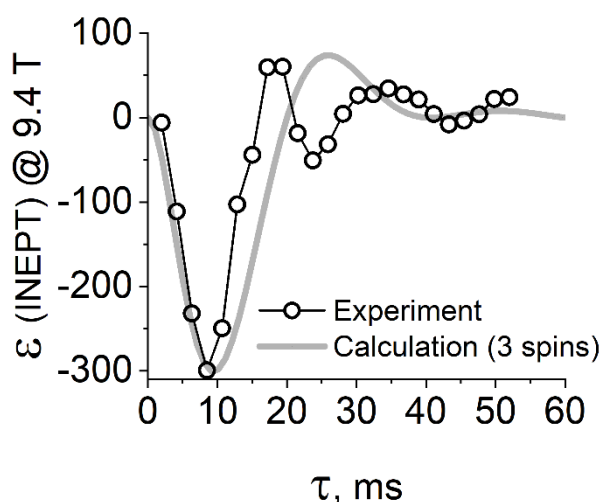


Figure S3. Dependence of the ^{15}N -SDAP signal enhancement on time delay τ introduced in the SABRE-INEPT pulse sequence (demonstrated in Fig. 1b of the main text). The experimental parameters: $\tau_1 = 10$ ms. The experimental data are represented as circles, whereas the theoretically calculated curve for a three-spin system is presented with a solid line.

The DRF-SABRE pulse sequence utilizes two continuous-wave (CW) magnetic fields exciting the nuclear spins of ^1H and ^{15}N nuclei in the polarization transfer complex, as demonstrated in Fig. S4. ^1H CW field is chosen to be on-resonant to the trans- ^1H hydride nuclei (trans-position is determined with respect to the complex-bound ^{15}N -SDAP) in the polarization transfer complex. In our case of ^{15}N -SDAP, the resonant position of this proton is equal to -23.72 ppm, which is RF excited, as demonstrated in Fig. S4, left. At the same time, ^{15}N CW field frequency is varied near the resonance of complex-bound ^{15}N -SDAP (242.37 ppm), as shown in Fig. S4, right. The dependence of the ^{15}N signal enhancement ε of ^{15}N -SDAP (free) on the frequency of the ^{15}N CW field is demonstrated in Fig. S5. The maximum absolute value of enhancement ε is observed at 241.87 ppm frequency of the ^{15}N CW field, which we have used in the subsequent experiments.

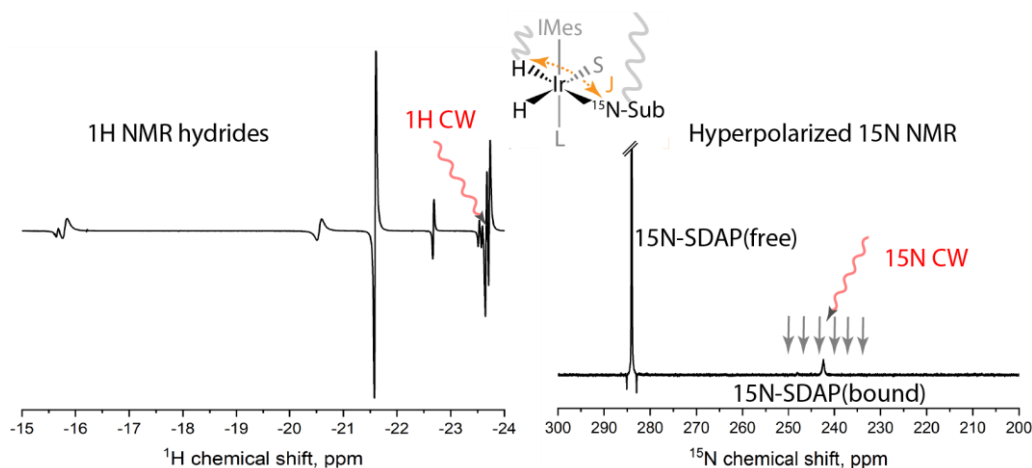


Figure S4. Visualization of the ^1H and ^{15}N frequencies excited in the DRF-SABRE experiment (demonstrated in Fig.1b, of the main text). (Left) ^1H CW is resonant towards hydride ^1H nucleus in its trans-position in the complex with respect to ^{15}N -sub. (right) ^{15}N CW frequency is varied near the resonant frequency of complex-bound ^{15}N -SDAP. The optimization of both RF fields leads to the hyperpolarization of ^{15}N -SDAP (free and bound).

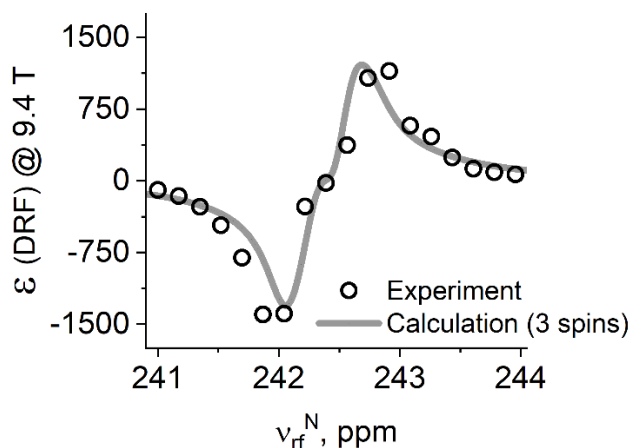


Figure S5. Dependence of the ^{15}N -SDAP signal enhancement on the ^{15}N CW frequency, ν_{rf}^N , in the DRF-SABRE experiment. The experimental parameters: the frequency of the ^1H CW field was fixed at $\nu_{rf}^H = -23.72$ ppm. The amplitudes of the CW fields were equal to 8 Hz. The experimental data are represented as circles, whereas the theoretically calculated curve for a three-spin system is a solid line.

References

1. A. N. Pravdivtsev, K. L. Ivanov, A. V. Yurkovskaya, P. A. Petrov, H.-H. Limbach, R. Kaptein, H.-M. Vieth, *J. Magn. Reson.*, **2015**, 261, 73–82. DOI: 10.1016/j.jmr.2015.10.006
2. C. R. Bowers, D. P. Weitekamp, *J. Am. Chem. Soc.*, **1987**, 109, 5541–5542. DOI: 10.1021/ja00252a049
3. R. W. Adams, J. A. Aguilar, K. D. Atkinson, M. J. Cowley, P. I. P. Elliott, S. B. Duckett, G. G. R. Green, I. G. Khazal, J. López-Serrano, D. C. Williamson, *Science*, **2009**, 323, 1708–1711. DOI: 10.1126/science.1168877
4. D. A. Barskiy, S. Knecht, A. V. Yurkovskaya, K. L. Ivanov, *Prog. Nucl. Magn. Reson. Spectrosc.*, **2019**, 114–115, 33–70. DOI: 10.1016/j.pnmrs.2019.05.005